

Functionally Graded Materials

*Nonlinear Analysis of
Plates and Shells*

Hui-Shen Shen



CRC Press
Taylor & Francis Group

Functionally Graded Materials

*Nonlinear Analysis of
Plates and Shells*

Functionally Graded Materials

*Nonlinear Analysis of
Plates and Shells*

Hui-Shen Shen



CRC Press

Taylor & Francis Group

Boca Raton London New York

CRC Press is an imprint of the
Taylor & Francis Group, an **informa** business

CRC Press
Taylor & Francis Group
6000 Broken Sound Parkway NW, Suite 300
Boca Raton, FL 33487-2742

© 2011 by Taylor & Francis Group, LLC
CRC Press is an imprint of Taylor & Francis Group, an Informa business

No claim to original U.S. Government works
Version Date: 20131120

International Standard Book Number-13: 978-1-4200-9257-8 (eBook - PDF)

This book contains information obtained from authentic and highly regarded sources. Reasonable efforts have been made to publish reliable data and information, but the author and publisher cannot assume responsibility for the validity of all materials or the consequences of their use. The authors and publishers have attempted to trace the copyright holders of all material reproduced in this publication and apologize to copyright holders if permission to publish in this form has not been obtained. If any copyright material has not been acknowledged please write and let us know so we may rectify in any future reprint.

Except as permitted under U.S. Copyright Law, no part of this book may be reprinted, reproduced, transmitted, or utilized in any form by any electronic, mechanical, or other means, now known or hereafter invented, including photocopying, microfilming, and recording, or in any information storage or retrieval system, without written permission from the publishers.

For permission to photocopy or use material electronically from this work, please access www.copyright.com (<http://www.copyright.com/>) or contact the Copyright Clearance Center, Inc. (CCC), 222 Rosewood Drive, Danvers, MA 01923, 978-750-8400. CCC is a not-for-profit organization that provides licenses and registration for a variety of users. For organizations that have been granted a photocopy license by the CCC, a separate system of payment has been arranged.

Trademark Notice: Product or corporate names may be trademarks or registered trademarks, and are used only for identification and explanation without intent to infringe.

Visit the Taylor & Francis Web site at
<http://www.taylorandfrancis.com>

and the CRC Press Web site at
<http://www.crcpress.com>

Contents

Preface.....	vii
Author.....	ix

Chapter 1 Modeling of Functionally Graded Materials and Structures	1
1.1 Introduction	1
1.2 Effective Material Properties of FGMs.....	3
1.3 Reddy's Higher Order Shear Deformation Plate Theory.....	9
1.4 Generalized Kármán-Type Nonlinear Equations	14
References.....	17

Chapter 2 Nonlinear Bending of Shear Deformable FGM Plates ...	21
2.1 Introduction	21
2.2 Nonlinear Bending of FGM Plates under Mechanical Loads in Thermal Environments	22
2.3 Nonlinear Thermal Bending of FGM Plates due to Heat Conduction.....	36
References.....	42

Chapter 3 Postbuckling of Shear Deformable FGM Plates	45
3.1 Introduction	45
3.2 Postbuckling of FGM Plates with Piezoelectric Actuators under Thermoelctromechanical Loads.....	47
3.3 Thermal Postbuckling Behavior of FGM Plates with Piezoelectric Actuators.....	66
3.4 Postbuckling of Sandwich Plates with FGM Face Sheets in Thermal Environments	82
References.....	96

Chapter 4 Nonlinear Vibration of Shear Deformable FGM Plates	99
4.1 Introduction	99
4.2 Nonlinear Vibration of FGM Plates in Thermal Environments	100
4.2.1 Free Vibration	108
4.2.2 Forced Vibration.....	108
4.3 Nonlinear Vibration of FGM Plates with Piezoelectric Actuators in Thermal Environments	118
4.4 Vibration of Postbuckled Sandwich Plates with FGM Face Sheets in Thermal Environments.....	132
References.....	143

- Chapter 5 Postbuckling of Shear Deformable FGM Shells** 147
- 5.1 Introduction 147
- 5.2 Boundary Layer Theory for the Buckling of FGM
Cylindrical Shells..... 149
 - 5.2.1 Donnell Theory 149
 - 5.2.2 Generalized Kármán–Donnell-Type Nonlinear Equations 150
 - 5.2.3 Boundary Layer-Type Equations 152
- 5.3 Postbuckling Behavior of FGM Cylindrical Shells
under Axial Compression 153
- 5.4 Postbuckling Behavior of FGM Cylindrical Shells
under External Pressure 169
- 5.5 Postbuckling Behavior of FGM Cylindrical Shells
under Torsion 183
- 5.6 Thermal Postbuckling Behavior of FGM
Cylindrical Shells..... 199
- References 208

- Appendix A**..... 211
- Appendix B** 213
- Appendix C** 215
- Appendix D** 221
- Appendix E** 225
- Appendix F** 227
- Appendix G** 229
- Appendix H** 231
- Appendix I** 233
- Appendix J** 235
- Appendix K**..... 239
- Appendix L** 241
- Appendix M**..... 245
- Appendix N** 247
- Appendix O** 257

- Index**..... 259

Preface

With the development of new industries and modern processes, many structures serve in thermal environments, resulting in a new class of composite materials called functionally graded materials (FGMs). FGMs were initially designed as thermal barrier materials for aerospace structural applications and fusion reactors. They are now developed for general use as structural components in extremely high-temperature environments. The ability to predict the response of FGM plates and shells when subjected to thermal and mechanical loads is of prime interest to structural analysis. In fact, many structures are subjected to high levels of load that may result in nonlinear load–deflection relationships due to large deformations. One of the important problems deserving special attention is the study of their nonlinear response to large deflection, postbuckling, and nonlinear vibration.

This book consists of five chapters. The chapter and section titles are significant indicators of the content matter. Each chapter contains adequate introductory material to enable engineering graduates who are familiar with the basic understanding of plates and shells to follow the text. The modeling of FGMs and structures is introduced and the derivation of the governing equations of FGM plates in the von Kármán sense is presented in Chapter 1. In Chapter 2, the geometrically nonlinear bending of FGM plates due to transverse static loads or heat conduction is presented. Chapter 3 furnishes a detailed treatment of the postbuckling problems of FGM plates subjected to thermal, electrical, and mechanical loads. Chapter 4 deals with the nonlinear vibration of FGM plates with or without piezoelectric actuators. Finally, Chapter 5 presents postbuckling solutions for FGM cylindrical shells under various loading conditions. Most of the solutions presented in these chapters are the results of investigations conducted by the author and his collaborators since 2001. The results presented herein may be treated as a benchmark for checking the validity and accuracy of other numerical solutions.

Despite a number of existing texts on the theory and analysis of plates and/or shells, there is not a single book that is devoted entirely to the geometrically nonlinear problems of inhomogeneous isotropic and functionally graded plates and shells. It is hoped that this book will fill the gap to some extent and be used as a valuable reference source for postgraduate students, engineers, scientists, and applied mathematicians in this field.

I wish to record my appreciation to the National Natural Science Foundation of China (grant nos. 59975058 and 50375091) for partially funding this work, and I also wish to thank my wife for her encouragement and forbearance.

Hui-Shen Shen

Author

Hui-Shen Shen is a professor of applied mechanics at Shanghai Jiao Tong University. He graduated from Tsinghua University in 1970, and received his MSc in solid mechanics and his PhD in structural mechanics from Shanghai Jiao Tong University in 1982 and 1986, respectively. In 1991–1992, he was a visiting research fellow at the University of Wales (Cardiff) and the University of Liverpool in the United Kingdom. Dr. Shen became a full professor of applied mechanics at Shanghai Jiao Tong University at the end of 1992. In 1995, he was invited again as a visiting professor at the University of Cardiff and in 1998–1999, as a visiting research fellow at the Hong Kong Polytechnic University, and in 2002–2003 as a visiting professor at the City University of Hong Kong. Also in 2002, he was a Tan Chin Tuan exchange fellow at the Nanyang Technological University in Singapore and in 2004, he was a Japan Society for the Promotion of Science (JSPS) invitation fellow at the Shizuoka University in Japan. In 2007, Dr. Shen was a visiting professor at the University of Western Sydney in Australia.

Dr. Shen's research interests include stability theory and, in general, non-linear response of plate and shell structures. He has published over 190 journal papers, of which 123 are international journal papers. His research publications have been widely cited in the areas of computational mechanics and structural engineering (more than 1500 times by papers published in 387 international archival journals, and 220 local journals, excluding self-citations). He is the coauthor of the books *Buckling of Structures* (with T.-Y. Chen) and *Postbuckling Behavior of Plates and Shells*. He won the second Science and Technology Progress Awards of Shanghai in 1998 and 2003, respectively. Currently, Dr. Shen serves on the editorial boards of the journal *Applied Mathematics and Mechanics* (ISSN: 0253-4827) and the *International Journal of Structural Stability and Dynamics* (ISSN: 0219-4554). He is a member of the American Society of Civil Engineers.

1

Modeling of Functionally Graded Materials and Structures

1.1 Introduction

The most lightweight composite materials with high strength/weight and stiffness/weight ratios have been used successfully in aircraft industry and other engineering applications. However, the traditional composite material is incapable to employ under the high-temperature environments. In general, the metals have been used in engineering field for many years on account of their excellent strength and toughness. In the high-temperature condition, the strength of the metal is reduced similar to the traditional composite material. The ceramic materials have excellent characteristics in heat resistance. However, the applications of ceramic are usually limited due to their low toughness.

Recently, a new class of composite materials known as functionally graded materials (FGMs) has drawn considerable attention. A typical FGM, with a high bending–stretching coupling effect, is an inhomogeneous composite made from different phases of material constituents (usually ceramic and metal). An example of such material is shown in Figure 1.1 (Yin et al. 2004) where spherical or nearly spherical particles are embedded within an isotropic matrix. Within FGMs the different microstructural phases have different functions, and the overall FGMs attain the multistructural status from their property gradation. By gradually varying the volume fraction of constituent materials, their material properties exhibit a smooth and continuous change from one surface to another, thus eliminating interface problems and mitigating thermal stress concentrations. This is due to the fact that the ceramic constituents of FGMs are able to withstand high-temperature environments due to their better thermal resistance characteristics, while the metal constituents provide stronger mechanical performance and reduce the possibility of catastrophic fracture.

The term FGMs was originated in the mid-1980s by a group of scientists in Japan (Yamanoushi et al. 1990, Koizumi 1993). Since then, an effort to develop high-resistant materials using FGMs had been continued. FGMs were initially designed as thermal barrier materials for aerospace structures and fusion reactors (Hirai and Chen 1999, Chan 2001, Uemura 2003). They

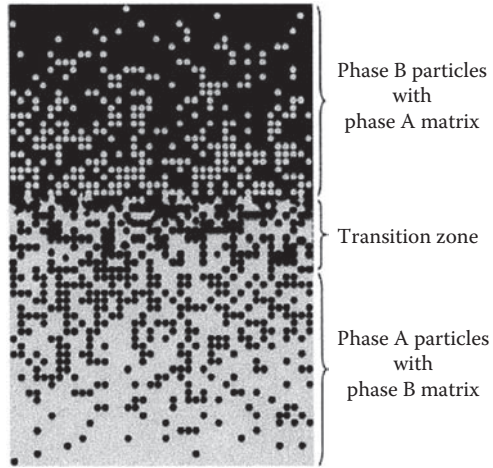


FIGURE 1.1
 An FGM with the volume fractions of constituent phases graded in one (vertical) direction. (From Yin, H.M., Sun, L.Z., and Paulino, G.H., *Acta Mater.*, 52, 3535, 2004. With permission.)

are now developed for the general use as structural components in high-temperature environments. An example is FGM thin-walled rotating blades as shown in Figure 1.2 (Librescu and Song 2005). Potential applications of FGM are both diverse and numerous. Applications of FGMs have recently been reported in the open literature, e.g., FGM sensors (Müller et al. 2003) and actuators (Qiu et al. 2003), FGM metal/ceramic armor (Liu et al. 2003), FGM photodetectors (Paszkievicz et al. 2008), and FGM dental implant (Watari et al. 2004, see Figure 1.3). A number of reviews dealing with various

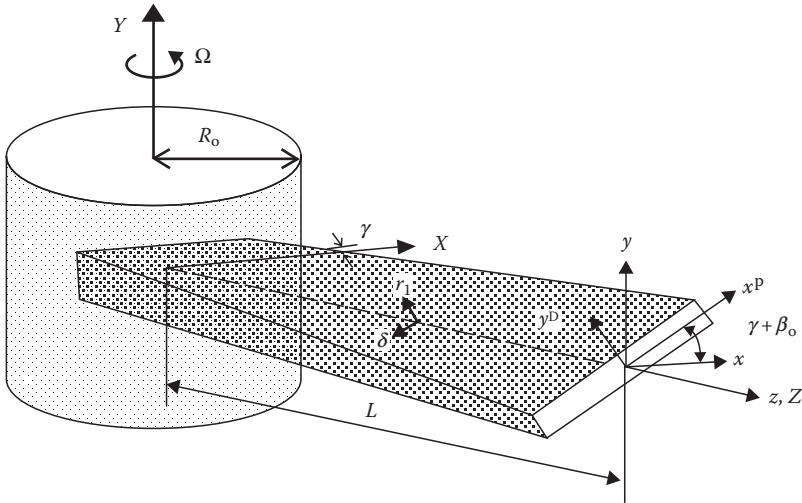


FIGURE 1.2
 An FGM thin-walled tapered pretwisted turbine blade. (From Librescu, L. and Song, S.-Y., *J. Therm. Stresses*, 28, 649, 2005. With permission.)

**FIGURE 1.3**

Ti/20HAP FGM dental implant. External appearance (left) and cross-section (right). (From Watari, F., Yokoyama, A., Omori, M., Hirai, T., Kondo, H., Uo, M., and Kawasaki, T., *Compos. Sci. Technol.*, 64, 893, 2004. With permission.)

aspects of FGMs have been published in the past few decades (Fuchiyama and Noda 1995, Markworth et al. 1995, Tanigawa 1995, Noda 1999, Paulino et al. 2003). They show that most of early research studies in FGMs had more focused on thermal stress analysis and fracture mechanics. A comprehensive survey for bending, buckling, and vibration analysis of plate and shell structures made of FGMs was presented by Shen (2004). Recently, Birman and Byrd (2007) presented a review of the principal developments in FGMs that includes heat transfer issues, stress, stability and dynamic analyses, testing, manufacturing and design, applications, and fracture.

1.2 Effective Material Properties of FGMs

Several FGMs are manufactured by two phases of materials with different properties. A detailed description of actual graded microstructures is usually not available, except perhaps for information on volume fraction distribution. Since the volume fraction of each phase gradually varies in the gradation direction, the effective properties of FGMs change along this direction. Therefore, we have two possible approaches to model FGMs. For the first choice, a piecewise variation of the volume fraction of ceramic or metal is assumed, and the FGM is taken to be layered with the same volume fraction in each region, i.e., quasihomogeneous ceramic–metal layers (Figure 1.4a). For the second choice, a continuous variation of the volume fraction of ceramic or metal is assumed (Figure 1.4b), and the metal volume fraction can be represented as the following function of the thickness coordinate Z .

$$V_m = \left(\frac{2Z + h}{2h} \right)^N \quad (1.1)$$

where h is the thickness of the structure, and N ($0 \leq N \leq \infty$) is a volume fraction exponent, which dictates the material variation profile through the

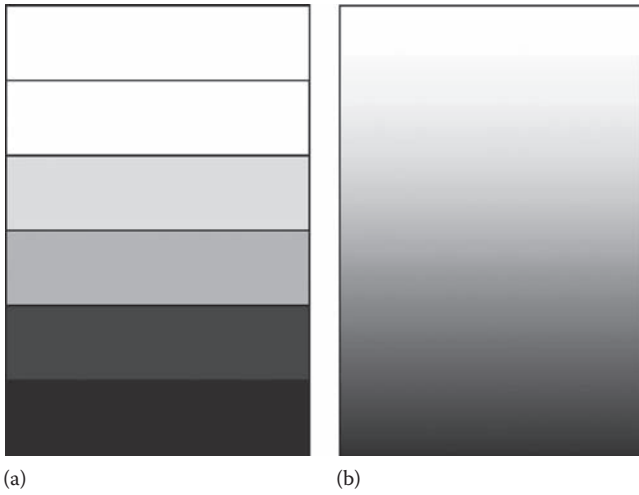


FIGURE 1.4
Analytical model for an FGM layer.

FGM layer thickness. As is presented in Figure 1.5, changing the value of N generates an infinite number of composition distributions.

In order to accurately model the material properties of FGMs, the properties must be temperature- and position-dependent. This is achieved by using

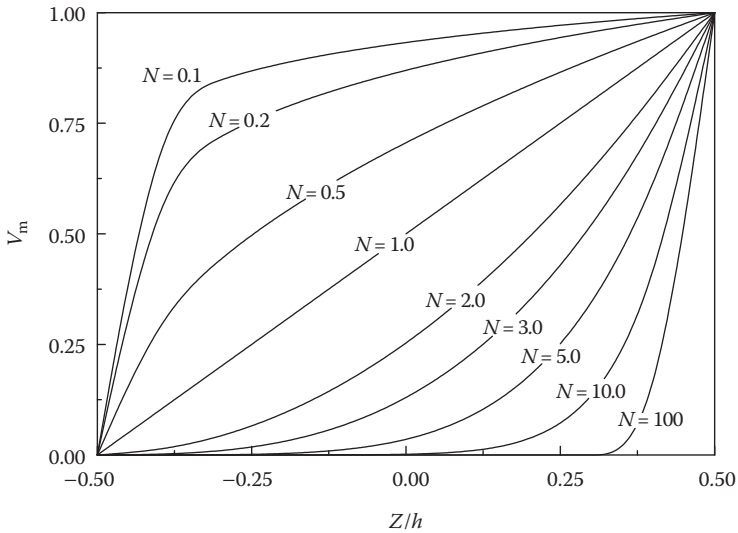


FIGURE 1.5
Volume fraction of metal along the thickness.

a simple rule of mixture of composite materials (Voigt model). The effective material properties P_f of the FGM layer, like Young's modulus E_f , and thermal expansion coefficient α_f , can then be expressed as

$$P_f = \sum_{j=1} P_j V_{f_j} \tag{1.2}$$

where P_j and V_{f_j} are the material properties and volume fraction of the constituent material j , and the sum of the volume fractions of all the constituent materials makes 1, i.e.,

$$\sum_{j=1} V_{f_j} = 1 \tag{1.3}$$

Since functionally graded structures are most commonly used in high-temperature environment where significant changes in mechanical properties of the constituent materials are to be expected (Reddy and Chin 1998), it is essential to take into consideration this temperature-dependency for accurate prediction of the mechanical response. Thus, the effective Young's modulus E_f , Poisson's ratio ν_f , thermal expansion coefficient α_f , and thermal conductivity κ_f are assumed to be temperature dependent and can be expressed as a non-linear function of temperature (Touloukian 1967):

$$P_j = P_0(P_{-1}T^{-1} + 1 + P_1T + P_2T^2 + P_3T^3) \tag{1.4}$$

where $P_0, P_{-1}, P_1, P_2,$ and P_3 are the coefficients of temperature T (in K) and are unique to the constituent materials. Typical values for Young's modulus E_f (in Pa), Poisson's ratio ν_f , thermal expansion coefficient α_f (in K^{-1}), and the thermal conductivity κ_f (in $W\ mK^{-1}$) of ceramics and metals are listed in Tables 1.1 through 1.4 (from Reddy and Chin 1998). From Equations 1.1 through 1.3, one has (Gibson et al. 1995):

$$E_f(Z, T) = [E_m(T) - E_c(T)] \left(\frac{2Z + h}{2h} \right)^N + E_c(T) \tag{1.5a}$$

TABLE 1.1

Modulus of Elasticity of Ceramics and Metals in Pa for E_f

Materials	P_0	P_{-1}	P_1	P_2	P_3
Zirconia	244.27e+9	0	-1.371e-3	1.214e-6	-3.681e-10
Aluminum oxide	349.55e+9	0	-3.853e-4	4.027e-7	-1.673e-10
Silicon nitride	348.43e+9	0	-3.070e-4	2.160e-7	-8.946e-11
Ti-6Al-4V	122.56e+9	0	-4.586e-4	0	0
Stainless steel	201.04e+9	0	3.079e-4	-6.534e-7	0
Nickel	223.95e+9	0	-2.794e-4	-3.998e-9	0

Source: Reddy, J.N. and Chin, C.D., *J. Therm. Stresses*, 21, 593, 1998. With permission.

TABLE 1.2

Coefficient of Thermal Expansion of Ceramics and Metals in K^{-1} for α_f

Materials	P_0	P_{-1}	P_1	P_2	P_3
Zirconia	12.766e - 6	0	-1.491e - 3	1.006e - 5	-6.778e - 11
Aluminum oxide	6.8269e - 6	0	1.838e - 4	0	0
Silicon nitride	5.8723e - 6	0	9.095e - 4	0	0
Ti-6Al-4V	7.5788e - 6	0	6.638e - 4	-3.147e - 6	0
Stainless steel	12.330e - 6	0	8.086e - 4	0	0
Nickel	9.9209e - 6	0	8.705e - 4	0	0

Source: Reddy, J.N. and Chin, C.D., *J. Therm. Stresses*, 21, 593, 1998. With permission.

TABLE 1.3

Thermal Conductivity of Ceramics and Metals in $W mK^{-1}$ for κ_f

Materials	P_0	P_{-1}	P_1	P_2	P_3
Zirconia	1.7000	0	1.276e - 4	6.648e - 8	0
Aluminum oxide	-14.087	-1123.6	-6.227e - 3	0	0
Silicon nitride	13.723	0	-1.032e - 3	5.466e - 7	-7.876e - 11
Ti-6Al-4V	1.0000	0	1.704e - 2	0	0
Stainless steel	15.379	0	-1.264e - 3	2.092e - 6	-7.223e - 10
Nickel ^a	187.66	0	-2.869e - 3	4.005e - 6	-1.983e - 9
Nickel ^b	58.754	0	-4.614e - 4	6.670e - 7	-1.523e - 10

Source: Reddy, J.N. and Chin, C.D., *J. Therm. Stresses*, 21, 593, 1998. With permission.

^a For $300 K \leq T \leq 635 K$.

^b For $635 K \leq T$.

TABLE 1.4

Poisson's Ratio of Ceramics and Metals for ν_f

Materials	P_0	P_{-1}	P_1	P_2	P_3
Zirconia	0.2882	0	1.133e - 4	0	0
Aluminum oxide	0.2600	0	0	0	0
Silicon nitride	0.2400	0	0	0	0
Ti-6Al-4V	0.2884	0	1.121e - 4	0	0
Stainless steel	0.3262	0	-2.002e - 4	3.797e - 7	0
Nickel	0.3100	0	0	0	0

Source: Reddy, J.N. and Chin, C.D., *J. Therm. Stresses*, 21, 593, 1998. With permission.

$$\alpha_f(Z, T) = [\alpha_m(T) - \alpha_c(T)] \left(\frac{2Z + h}{2h} \right)^N + \alpha_c(T) \quad (1.5b)$$

$$\kappa_f(Z, T) = [\kappa_m(T) - \kappa_c(T)] \left(\frac{2Z + h}{2h} \right)^N + \kappa_c(T) \quad (1.5c)$$

$$\nu_f(Z, T) = [\nu_m(T) - \nu_c(T)] \left(\frac{2Z + h}{2h} \right)^N + \nu_c(T) \quad (1.5d)$$

It is evident that E_f , ν_f , α_f , and κ_f are both temperature- and position-dependent. This method is simple and convenient to apply for predicting the overall material properties and responses; however, owing to the assumed simplifications the validity is affected by the detailed graded microstructure.

As argued before, precise information about the size, the shape, and the distribution of particles is not available and the effective elastic moduli of the graded microstructures must be evaluated based on the volume fraction distribution and the approximate shape of the dispersed phase. Several micromechanics models have also been developed over the years to infer the effective properties of FGMs. The Mori–Tanaka scheme (Mori and Tanaka 1973, Benveniste 1987) for estimating the effective moduli is applicable to regions of the graded microstructure which have a well-defined continuous matrix and a discontinuous particulate phase as depicted in Figure 1.1. It takes into account the interaction of the elastic fields among neighboring inclusions. It is assumed that the matrix phase, denoted by the subscript 1, is reinforced by spherical particles of a particulate phase, denoted by the subscript 2. In this notation, K_1 , G_1 , and V_1 denote, respectively, the bulk modulus, the shear modulus, and the volume fraction of the matrix phase; K_2 , G_2 , and V_2 denote the corresponding material properties and the volume fraction of the particulate phase. It should be noted that $V_1 + V_2 = 1$. The effective local bulk modulus K_f , the shear modulus G_f , thermal expansion coefficient α_f , and thermal conductivity κ_f obtained by the Mori–Tanaka scheme for a random distribution of isotropic particles in an isotropic matrix are given by

$$\frac{K_f - K_1}{K_2 - K_1} = \frac{V_2}{1 + (1 - V_2)(3(K_2 - K_1)/(3K_1 + 4G_1))} \quad (1.6a)$$

$$\frac{G_f - G_1}{G_2 - G_1} = \frac{V_2}{1 + (1 - V_2)((G_2 - G_1)/(G_1 + f_1))} \quad (1.6b)$$

$$\frac{\alpha_f - \alpha_1}{\alpha_2 - \alpha_1} = \frac{(1/K_f) - (1/K_1)}{(1/K_2) - (1/K_1)} \quad (1.6c)$$

$$\frac{\kappa_f - \kappa_1}{\kappa_2 - \kappa_1} = \frac{V_2}{1 + (1 - V_2)((\kappa_2 - \kappa_1)/3\kappa_1)} \quad (1.6d)$$

where

$$f_1 = \frac{G_1(9K_1 + 8G_1)}{6(K_1 + 2G_1)} \quad (1.7)$$

The self-consistent method (Hill 1965) assumes that each reinforcement inclusion is embedded in a continuum material whose effective properties are those of the composite. This method does not distinguish between matrix and reinforcement phases and the same overall moduli are predicted in another composite in which the roles of the phases are interchanged. This makes it particularly suitable for determining the effective moduli in those regions which have an interconnected skeletal microstructure as depicted in Figure 1.6. The locally effective elastic moduli by the self-consistent method are given by

$$\frac{\delta}{K_f} = \frac{V_1}{K_f - K_2} + \frac{V_2}{K_f - K_1} \quad (1.8a)$$

$$\frac{\eta}{G_f} = \frac{V_1}{G_f - G_2} + \frac{V_2}{G_f - G_1} \quad (1.8b)$$

where

$$\delta = 3 - 5\eta = \frac{K_f}{K_f + (4/3)G_f} \quad (1.9)$$



FIGURE 1.6 Skeletal microstructure of FGM material. (From Vel, S.S. and Batra, R.C., *AIAA J.*, 40, 1421, 2002. With permission.)

From Equation 1.8a, one has

$$K_f = \frac{1}{(V_1/(K_1 + (4/3)G_f)) + (V_2/(K_2 + (4/3)G_f))} - \frac{4}{3}G_f \quad (1.10)$$

and G_f is obtained by solving the following quartic equation:

$$\begin{aligned} & [V_1K_1/(K_1 + 4G_f/3) + V_2K_2/(K_2 + 4G_f/3)] \\ & + 5[V_1G_2/(G_f - G_2) + V_2G_1/(G_f - G_1)] + 2 = 0 \end{aligned} \quad (1.11)$$

Then, the effective Young's modulus E_f and Poisson's ratio ν_f can be found from $E_f = 9K_fG_f/3K_f + G_f$ and $\nu_f = (3K_f - 2G_f)/2(3K_f + G_f)$, respectively.

A comparison between the Mori–Tanaka and self-consistent models and the finite element simulation of FGM was presented in Reuter et al. (1997) and Reuter and Dvorak (1998). The Mori–Tanaka model was shown to yield accurate prediction of the properties with a well-defined continuous matrix and discontinuous inclusions, while the self-consistent model was better in skeletal microstructures characterized by a wide transition zone between the regions with predominance of one of the constituent phases.

1.3 Reddy's Higher Order Shear Deformation Plate Theory

Reddy (1984a,b) developed a simple higher order shear deformation plate theory (HSDPT), in which the transverse shear strains are assumed to be parabolically distributed across the plate thickness. The theory is simple in the sense that it contains the same dependent unknowns as in the first-order shear deformation plate theory (FSDPT), and no shear correction factors are required.

Consider a rectangular plate made of FGMs. The length, width, and total thickness of the plate are a , b , and h . As usual, the coordinate system has its origin at the corner of the plate on the midplane. Let \bar{U} , \bar{V} , and \bar{W} be the plate displacements parallel to a right-hand set of axes (X, Y, Z) , where X is longitudinal and Z is perpendicular to the plate. $\bar{\Psi}_x$ and $\bar{\Psi}_y$ are the midplane rotations of the normal about the Y and X axes, respectively. The displacement components are assumed to be of the following form:

$$U_1 = \bar{U}(X, Y, t) + Z\bar{\Psi}_x(X, Y, t) + Z^2\xi_x(X, Y, t) + Z^3\zeta_x(X, Y, t) \quad (1.12a)$$

$$U_2 = \bar{V}(X, Y, t) + Z\bar{\Psi}_y(X, Y, t) + Z^2\xi_y(X, Y, t) + Z^3\zeta_y(X, Y, t) \quad (1.12b)$$

$$U_3 = \bar{W}(X, Y, t) \quad (1.12c)$$

where t represents time, \bar{U} , \bar{V} , \bar{W} , $\bar{\Psi}_x$, $\bar{\Psi}_y$, $\bar{\xi}_x$, $\bar{\xi}_y$, $\bar{\zeta}_x$, and $\bar{\zeta}_y$ are unknowns.

If the transverse shear stresses σ_4 and σ_5 are to vanish at the bounding planes of the plate (at $Z = \pm h/2$), the transverse shear strains ε_4 and ε_5 should also vanish there. That is

$$\varepsilon_5\left(X, Y, \pm \frac{h}{2}, t\right) = 0, \quad \varepsilon_4\left(X, Y, \pm \frac{h}{2}, t\right) = 0 \quad (1.13)$$

which imply the following conditions

$$\bar{\xi}_x = 0 \quad (1.14a)$$

$$\bar{\xi}_y = 0 \quad (1.14b)$$

$$\bar{\zeta}_x = -\frac{4}{3h^2} \left(\frac{\partial \bar{W}}{\partial X} + \bar{\Psi}_x \right) \quad (1.14c)$$

$$\bar{\zeta}_y = -\frac{4}{3h^2} \left(\frac{\partial \bar{W}}{\partial Y} + \bar{\Psi}_y \right) \quad (1.14d)$$

Putting the above conditions in Equation 1.12 leads to the following displacement field

$$U_1 = \bar{U} + 2 \left[\bar{\Psi}_x - \chi \frac{4}{3} \left(\frac{2}{h} \right)^2 \left(\bar{\Psi}_x + \frac{\partial \bar{W}}{\partial X} \right) \right] \quad (1.15a)$$

$$U_2 = \bar{V} + 2 \left[\bar{\Psi}_y - \chi \frac{4}{3} \left(\frac{2}{h} \right)^2 \left(\bar{\Psi}_y + \frac{\partial \bar{W}}{\partial Y} \right) \right] \quad (1.15b)$$

$$U_3 = \bar{W} \quad (1.15c)$$

in which χ is a tracer. If $\chi = 1$, Equation 1.15 is for the case of the HSDPT, which contains the same dependent unknowns (\bar{U} , \bar{V} , \bar{W} , $\bar{\Psi}_x$, and $\bar{\Psi}_y$) as in the FSDPT. If $\chi = 0$, Equation 1.15 is reduced to the case of the FSDPT.

The strains of the plate associated with the displacement field given in Equation 1.15 are

$$\begin{aligned} \varepsilon_1 &= \varepsilon_1^0 + Z(\kappa_1^0 + Z^2 \kappa_1^2) \\ \varepsilon_2 &= \varepsilon_2^0 + Z(\kappa_2^0 + Z^2 \kappa_2^2) \\ \varepsilon_3 &= 0 \\ \varepsilon_4 &= \varepsilon_4^0 + Z^2 \kappa_4^2 \\ \varepsilon_5 &= \varepsilon_5^0 + Z^2 \kappa_5^2 \\ \varepsilon_6 &= \varepsilon_6^0 + Z(\kappa_6^0 + Z^2 \kappa_6^2) \end{aligned} \quad (1.16)$$

where

$$\begin{aligned}
 \varepsilon_1^0 &= \frac{\partial \bar{U}}{\partial X} + \frac{1}{2} \left(\frac{\partial \bar{W}}{\partial X} \right)^2, & \kappa_1^0 &= \frac{\partial \bar{\Psi}_x}{\partial X}, & \kappa_1^2 &= -\chi \frac{4}{3h^2} \left(\frac{\partial \bar{\Psi}_x}{\partial X} + \frac{\partial^2 \bar{W}}{\partial X^2} \right) \\
 \varepsilon_2^0 &= \frac{\partial \bar{V}}{\partial Y} + \frac{1}{2} \left(\frac{\partial \bar{W}}{\partial Y} \right)^2, & \kappa_2^0 &= \frac{\partial \bar{\Psi}_y}{\partial Y}, & \kappa_2^2 &= -\chi \frac{4}{3h^2} \left(\frac{\partial \bar{\Psi}_y}{\partial Y} + \frac{\partial^2 \bar{W}}{\partial Y^2} \right) \\
 \varepsilon_4^0 &= \bar{\Psi}_y + \frac{\partial \bar{W}}{\partial Y}, & \kappa_4^2 &= -\chi \frac{4}{h^2} \left(\bar{\Psi}_y + \frac{\partial \bar{W}}{\partial Y} \right) \\
 \varepsilon_5^0 &= \bar{\Psi}_x + \frac{\partial \bar{W}}{\partial X}, & \kappa_5^2 &= -\chi \frac{4}{h^2} \left(\bar{\Psi}_x + \frac{\partial \bar{W}}{\partial X} \right) \\
 \varepsilon_6^0 &= \frac{\partial \bar{U}}{\partial Y} + \frac{\partial \bar{V}}{\partial X} + \frac{\partial \bar{W}}{\partial X} \frac{\partial \bar{W}}{\partial Y} \\
 \kappa_6^0 &= \frac{\partial \bar{\Psi}_x}{\partial Y} + \frac{\partial \bar{\Psi}_y}{\partial X} \\
 \kappa_6^2 &= -\chi \frac{4}{3h^2} \left(\frac{\partial \bar{\Psi}_x}{\partial Y} + \frac{\partial \bar{\Psi}_y}{\partial X} + 2 \frac{\partial^2 \bar{W}}{\partial X \partial Y} \right)
 \end{aligned} \tag{1.17}$$

The plane stress constitutive equations may then be written in the form:

$$\begin{bmatrix} \sigma_1 \\ \sigma_2 \\ \sigma_6 \end{bmatrix} = \begin{bmatrix} Q_{11} & Q_{12} & 0 \\ Q_{21} & Q_{22} & 0 \\ 0 & 0 & Q_{66} \end{bmatrix} \begin{bmatrix} \varepsilon_1 \\ \varepsilon_2 \\ \varepsilon_6 \end{bmatrix} \tag{1.18a}$$

$$\begin{bmatrix} \sigma_4 \\ \sigma_5 \end{bmatrix} = \begin{bmatrix} Q_{44} & 0 \\ 0 & Q_{55} \end{bmatrix} \begin{bmatrix} \varepsilon_4 \\ \varepsilon_5 \end{bmatrix} \tag{1.18b}$$

where Q_{ij} are the transformed reduced stiffnesses defined by

$$\begin{aligned}
 Q_{11} = Q_{22} &= \frac{E_f(Z, T)}{1 - \nu_f^2}, & Q_{12} &= \frac{\nu_f E_f(Z, T)}{1 - \nu_f^2}, \\
 Q_{16} = Q_{26} &= 0, & Q_{44} = Q_{55} = Q_{66} &= \frac{E_f(Z, T)}{2(1 + \nu_f)}
 \end{aligned} \tag{1.19}$$

As in the classical plate theory, the stress resultants and couples are defined by

$$(\bar{N}_i, \bar{M}_i, \bar{P}_i) = \int_{-h/2}^{h/2} \sigma_i(1, Z, Z^3) dZ, \quad i = 1, 2, 6 \tag{1.20a}$$

$$(\bar{Q}_2, \bar{R}_2) = \int_{-h/2}^{h/2} \sigma_4(1, Z^2) dZ \tag{1.20b}$$

$$(\bar{Q}_1, \bar{R}_1) = \int_{-h}^h \sigma_3(1, Z^2) dZ \quad (1.20c)$$

where

\bar{N}_i and \bar{Q}_i are the membrane and transverse shear forces
 \bar{M}_i is the bending moment per unit length
 \bar{P}_i and \bar{R}_i are the higher order bending moment and shear force,
 respectively

Substituting Equation 1.18 into Equation 1.20, and taking Equation 1.16 into account, yields the constitutive relations of the plate

$$\begin{bmatrix} \bar{N} \\ \bar{M} \\ \bar{P} \end{bmatrix} = \begin{bmatrix} A & B & E \\ B & D & F \\ E & F & H \end{bmatrix} \begin{bmatrix} \boldsymbol{\varepsilon}^0 \\ \boldsymbol{\kappa}^0 \\ \boldsymbol{\kappa}^2 \end{bmatrix} \quad (1.21a)$$

$$\begin{bmatrix} \bar{Q} \\ \bar{R} \end{bmatrix} = \begin{bmatrix} A & D \\ D & F \end{bmatrix} \begin{bmatrix} \boldsymbol{\varepsilon}^0 \\ \boldsymbol{\kappa}^2 \end{bmatrix} \quad (1.21b)$$

where A_{ij} , B_{ij} , etc. are the plate stiffnesses, defined by

$$(A_{ij}, B_{ij}, D_{ij}, E_{ij}, F_{ij}, H_{ij}) = \int_{-h/2}^{+h/2} (Q_{ij})(1, Z, Z^2, Z^3, Z^4, Z^6) dZ, \quad i, j = 1, 2, 6 \quad (1.22a)$$

$$(A_{ij}, D_{ij}, F_{ij}) = \int_{-h/2}^{+h/2} (Q_{ij})(1, Z^2, Z^4) dZ, \quad i, j = 4, 5 \quad (1.22b)$$

The Hamilton principle for an elastic body is

$$\int_{t_1}^{t_2} (\delta U + \delta V - \delta K) dt = 0 \quad (1.23)$$

where

δU is the virtual strain energy
 δV is the virtual work done by external forces
 δK is the virtual kinetic energy

$$\begin{aligned} \delta U &= \int_{\Omega} \int_{-h/2}^{h/2} (\sigma_i \delta \varepsilon_i) dZ dX dY \\ &= \int_{\Omega} (\bar{N}_i \delta \varepsilon_i^0 + \bar{M}_i \delta \kappa_i^0 + \bar{P}_i \delta \kappa_i^2) dZ dX dY, \quad i = 1, 2, 6 \end{aligned} \quad (1.24a)$$

$$\delta V = - \int_{\Omega} [q(X, Y)\delta U_3]dX dY \quad (1.24b)$$

$$\delta K = \int_{\Omega} \int_{-h/2}^{h/2} \rho(\dot{U}_j\delta\dot{U}_j)dZ dX dY, \quad j = 1, 2, 3 \quad (1.24c)$$

In Equation 1.24c, the superposed dots indicate differentiation with respect to time. Integrating Equation 1.23, and collecting the coefficients of $\delta\bar{U}$, $\delta\bar{V}$, $\delta\bar{W}$, $\delta\bar{\Psi}_x$, and $\delta\bar{\Psi}_y$, we obtain the following equations of motion

$$\begin{aligned} \delta\bar{U}: \frac{\partial\bar{N}_1}{\partial X} + \frac{\partial\bar{N}_6}{\partial Y} &= I_1 \frac{\partial^2\bar{U}}{\partial t^2} + \bar{I}_2 \frac{\partial^2\bar{\Psi}_x}{\partial t^2} - c_1 I_4 \frac{\partial^3\bar{W}}{\partial X\partial t^2} \\ \delta\bar{V}: \frac{\partial\bar{N}_6}{\partial X} + \frac{\partial\bar{N}_2}{\partial Y} &= I_1 \frac{\partial^2\bar{V}}{\partial t^2} + \bar{I}_2 \frac{\partial^2\bar{\Psi}_y}{\partial t^2} - c_1 I_4 \frac{\partial^3\bar{W}}{\partial Y\partial t^2} \\ \delta\bar{W}: \frac{\partial\bar{Q}_1}{\partial X} + \frac{\partial\bar{Q}_2}{\partial Y} + \frac{\partial}{\partial X} \left(\bar{N}_1 \frac{\partial\bar{W}}{\partial X} + \bar{N}_6 \frac{\partial\bar{W}}{\partial Y} \right) + \frac{\partial}{\partial Y} \left(\bar{N}_6 \frac{\partial\bar{W}}{\partial X} + \bar{N}_2 \frac{\partial\bar{W}}{\partial Y} \right) \\ &+ q - c_2 \left(\frac{\partial\bar{R}_1}{\partial X} + \frac{\partial\bar{R}_2}{\partial Y} \right) + c_1 \left(\frac{\partial^2\bar{P}_1}{\partial X^2} + 2 \frac{\partial^2\bar{P}_6}{\partial X\partial Y} + \frac{\partial^2\bar{P}_2}{\partial Y^2} \right) \\ &= I_1 \frac{\partial^2\bar{W}}{\partial t^2} - c_1^2 I_7 \frac{\partial^2}{\partial t^2} \left(\frac{\partial^2\bar{W}}{\partial X^2} + \frac{\partial^2\bar{W}}{\partial Y^2} \right) + c_1 I_4 \frac{\partial^2}{\partial t^2} \left(\frac{\partial\bar{U}}{\partial X} + \frac{\partial\bar{V}}{\partial Y} \right) + c_1 \bar{I}_5 \frac{\partial^2}{\partial t^2} \left(\frac{\partial\bar{\Psi}_x}{\partial X} + \frac{\partial\bar{\Psi}_y}{\partial Y} \right) \\ \delta\bar{\Psi}_x: \frac{\partial\bar{M}_1}{\partial X} + \frac{\partial\bar{M}_6}{\partial Y} - \bar{Q}_1 + C_2\bar{R}_1 - C_1 \left(\frac{\partial\bar{P}_1}{\partial X} + \frac{\partial\bar{P}_6}{\partial Y} \right) &= \bar{I}_2 \frac{\partial^2\bar{U}}{\partial t^2} + \bar{I}_3 \frac{\partial^2\bar{\Psi}_x}{\partial t^2} - c_1 \bar{I}_5 \frac{\partial^3\bar{W}}{\partial X\partial t^2} \\ \delta\bar{\Psi}_y: \frac{\partial\bar{M}_6}{\partial X} + \frac{\partial\bar{M}_2}{\partial Y} - \bar{Q}_2 + c_2\bar{R}_2 - c_1 \left(\frac{\partial\bar{P}_6}{\partial X} + \frac{\partial\bar{P}_2}{\partial Y} \right) &= \bar{I}_2 \frac{\partial^2\bar{V}}{\partial t^2} + \bar{I}_3 \frac{\partial^2\bar{\Psi}_y}{\partial t^2} - c_1 \bar{I}_5 \frac{\partial^3\bar{W}}{\partial Y\partial t^2} \end{aligned} \quad (1.25)$$

where $c_1 = 4/3h^2$, $c_2 = 3c_1$, and

$$\bar{I}_2 = I_2 - c_1 I_4, \quad \bar{I}_5 = I_5 - c_1 I_7, \quad \bar{I}_3 = I_3 - 2c_1 I_5 + c_1^2 I_7, \quad \bar{I}_8 = \bar{I}_3 + \bar{I}_5 \quad (1.26a)$$

and the inertias I_i ($i = 1, 2, 3, 4, 5, 7$) are defined by

$$(I_1, I_2, I_3, I_4, I_5, I_7) = \int_{-h/2}^{h/2} \rho(Z)(1, Z, Z^2, Z^3, Z^4, Z^6)dZ \quad (1.26b)$$

where ρ is the mass density of the plate, which may also be position dependent.

1.4 Generalized Kármán-Type Nonlinear Equations

Based on Reddy’s HSDPT with a von Kármán-type of kinematic nonlinearity (Reddy 1984b) and including thermal effects, Shen (1997) derived a set of general von Kármán-type equations which can be expressed in terms of a stress function \bar{F} , two rotations $\bar{\Psi}_x$ and $\bar{\Psi}_y$, and a transverse displacement \bar{W} , along with the initial geometric imperfection \bar{W}^* . These equations are then extended to the case of shear deformable FGM plates.

Let $\bar{F}(X, Y)$ be the stress function for the stress resultants defined by $\bar{N}_x = \bar{F}_{,yy}$, $\bar{N}_y = \bar{F}_{,xx}$, and $\bar{N}_{xy} = -\bar{F}_{,xy}$, where a comma denotes partial differentiation with respect to the corresponding coordinates.

If thermal effect is taken into account, we assume

$$N^* = \bar{N} - \bar{N}^T, \quad M^* = \bar{M} - \bar{M}^T, \quad P^* = \bar{P} - \bar{P}^T \quad (1.27)$$

where \bar{N}^T , \bar{M}^T , \bar{S}^T , and \bar{P}^T are the forces, moments, and higher order moments caused by elevated temperature, and are defined by

$$\begin{bmatrix} \bar{N}_x^T & \bar{M}_x^T & \bar{P}_x^T \\ \bar{N}_y^T & \bar{M}_y^T & \bar{P}_y^T \\ \bar{N}_{xy}^T & \bar{M}_{xy}^T & \bar{P}_{xy}^T \end{bmatrix} = \int_{-h/2}^{+h/2} \begin{bmatrix} A_x \\ A_y \\ A_{xy} \end{bmatrix} (1, Z, Z^3) \Delta T(X, Y, Z) dZ \quad (1.28a)$$

$$\begin{bmatrix} \bar{S}_x^T \\ \bar{S}_y^T \\ \bar{S}_{xy}^T \end{bmatrix} = \begin{bmatrix} \bar{M}_x^T \\ \bar{M}_y^T \\ \bar{M}_{xy}^T \end{bmatrix} - \frac{4}{3h^2} \begin{bmatrix} \bar{P}_x^T \\ \bar{P}_y^T \\ \bar{P}_{xy}^T \end{bmatrix} \quad (1.28b)$$

where $\Delta T(X, Y, Z) = T(X, Y, Z) - T_0$ is temperature rise from the reference temperature T_0 at which there are no thermal strains, and

$$\begin{bmatrix} A_x \\ A_y \\ A_{xy} \end{bmatrix} = - \begin{bmatrix} Q_{11} & Q_{12} & Q_{16} \\ Q_{12} & Q_{22} & Q_{26} \\ Q_{16} & Q_{26} & Q_{66} \end{bmatrix} \begin{bmatrix} 1 & 0 \\ 0 & 1 \\ 0 & 0 \end{bmatrix} \begin{bmatrix} \alpha_{11} \\ \alpha_{22} \end{bmatrix} \quad (1.29)$$

where α_{11} and α_{22} are the thermal expansion coefficients measured in the longitudinal and transverse directions, respectively.

The partial inverse of Equation 1.21a yields

$$\begin{bmatrix} \epsilon^0 \\ M^* \\ P^* \end{bmatrix} = \begin{bmatrix} A^* & B^* & E^* \\ -(B^*)^T & D^* & (F^*)^T \\ -(E^*)^T & F^* & H^* \end{bmatrix} \begin{bmatrix} N^* \\ \kappa^0 \\ \kappa^2 \end{bmatrix} \quad (1.30)$$

where the superscript “T” represents the matrix transpose and in which the reduced stiffness matrices $[A_{ij}^*]$, $[B_{ij}^*]$, $[D_{ij}^*]$, $[E_{ij}^*]$, $[F_{ij}^*]$, and $[H_{ij}^*]$ ($i, j = 1, 2, 6$) are functions of temperature and position, determined through relationships (Shen 1997):

$$\begin{aligned} A^* &= A^{-1}, \quad B^* = -A^{-1}B, \quad D^* = D - BA^{-1}B, \quad E^* = -A^{-1}E, \\ F^* &= F - EA^{-1}B, \quad H^* = H - EA^{-1}E \end{aligned} \quad (1.31)$$

From Equation 1.30, the bending moments, higher order moments, and transverse shear forces can be written in the form:

$$\begin{aligned} \bar{M}_x = \bar{M}_1 &= -B_{11}^* \bar{F}_{,yy} - B_{21}^* \bar{F}_{,xx} + D_{11}^* \bar{\Psi}_{x,rx} + D_{12}^* \bar{\Psi}_{y,ry} \\ &\quad - c_1 [F_{11}^* (\bar{\Psi}_{x,rx} + \bar{W}_{,rx}) + F_{21}^* (\bar{\Psi}_{y,ry} + \bar{W}_{,yy})] + \bar{M}_x^T \end{aligned} \quad (1.32a)$$

$$\begin{aligned} \bar{M}_y = \bar{M}_2 &= -B_{12}^* \bar{F}_{,yy} - B_{22}^* \bar{F}_{,xx} + D_{12}^* \bar{\Psi}_{x,rx} + D_{22}^* \bar{\Psi}_{y,ry} \\ &\quad - c_1 [F_{12}^* (\bar{\Psi}_{x,rx} + \bar{W}_{,rx}) + F_{22}^* (\bar{\Psi}_{y,ry} + \bar{W}_{,yy})] + \bar{M}_y^T \end{aligned} \quad (1.32b)$$

$$\begin{aligned} \bar{M}_{xy} = \bar{M}_6 &= B_{66}^* \bar{F}_{,xy} + D_{66}^* (\bar{\Psi}_{x,ry} + \bar{\Psi}_{y,rx}) \\ &\quad - c_1 F_{66}^* (\bar{\Psi}_{x,ry} + \bar{\Psi}_{y,rx} + 2\bar{W}_{,xy}) + \bar{M}_{xy}^T \end{aligned} \quad (1.32c)$$

$$\begin{aligned} \bar{P}_x = \bar{P}_1 &= -E_{11}^* \bar{F}_{,yy} - E_{21}^* \bar{F}_{,xx} + F_{11}^* \bar{\Psi}_{x,rx} + F_{12}^* \bar{\Psi}_{y,ry} \\ &\quad - c_1 [H_{11}^* (\bar{\Psi}_{x,rx} + \bar{W}_{,rx}) + H_{12}^* (\bar{\Psi}_{y,ry} + \bar{W}_{,yy})] + \bar{P}_x^T \end{aligned} \quad (1.32d)$$

$$\begin{aligned} \bar{P}_y = \bar{P}_2 &= -E_{12}^* \bar{F}_{,yy} - E_{22}^* \bar{F}_{,xx} + F_{21}^* \bar{\Psi}_{x,rx} + D_{22}^* \bar{\Psi}_{y,ry} \\ &\quad - c_1 [H_{12}^* (\bar{\Psi}_{x,rx} + \bar{W}_{,rx}) + H_{22}^* (\bar{\Psi}_{y,ry} + \bar{W}_{,yy})] + \bar{P}_y^T \end{aligned} \quad (1.32e)$$

$$Q_1 = (A_{55} - c_2 D_{55}) (\bar{\Psi}_x + \bar{W}_{,x}) \quad (1.32f)$$

$$R_1 = (D_{55} - c_2 F_{55}) (\bar{\Psi}_x + \bar{W}_{,x}) \quad (1.32g)$$

$$Q_2 = (A_{44} - c_2 D_{44}) (\bar{\Psi}_y + \bar{W}_{,y}) \quad (1.32h)$$

$$R_2 = (D_{44} - c_2 F_{44}) (\bar{\Psi}_y + \bar{W}_{,y}) \quad (1.32i)$$

Substituting Equation 1.32 into Equation 1.25, and considering the condition of compatibility, which is also expressed in terms of \bar{F} , $\bar{\Psi}_x$, $\bar{\Psi}_y$, \bar{W} , and \bar{W}^* , the equations of motion are obtained in the following

$$\begin{aligned} &\tilde{L}_{11}(\bar{W}) - \tilde{L}_{12}(\bar{\Psi}_x) - \tilde{L}_{13}(\bar{\Psi}_y) + \tilde{L}_{14}(\bar{F}) - \tilde{L}_{15}(\bar{N}^T) - \tilde{L}_{16}(\bar{M}^T) \\ &= \tilde{L}(\bar{W} + \bar{W}^*, \bar{F}) + \tilde{L}_{17}(\ddot{\bar{W}}) - \tilde{I}_8(\ddot{\bar{\Psi}}_{x,rx} + \ddot{\bar{\Psi}}_{y,ry}) + q \end{aligned} \quad (1.33)$$

$$\tilde{L}_{21}(\bar{F}) + \tilde{L}_{22}(\bar{\Psi}_x) + \tilde{L}_{23}(\bar{\Psi}_y) - \tilde{L}_{24}(\bar{W}) - \tilde{L}_{25}(\bar{N}^T) = -\frac{1}{2} \tilde{L}(\bar{W} + 2\bar{W}^*, \bar{W}) \quad (1.34)$$

$$\begin{aligned} & \tilde{L}_{31}(\bar{W}) + \tilde{L}_{32}(\bar{\Psi}_x) - \tilde{L}_{33}(\bar{\Psi}_y) + \tilde{L}_{34}(\bar{F}) - \tilde{L}_{35}(\bar{N}^T) - \tilde{L}_{36}(\bar{S}^T) \\ & = \bar{I}_5 \ddot{\bar{W}}_{,x} - \bar{I}_3 \ddot{\bar{\Psi}}_x \end{aligned} \quad (1.35)$$

$$\begin{aligned} & \tilde{L}_{41}(\bar{W}) - \tilde{L}_{42}(\bar{\Psi}_x) + \tilde{L}_{43}(\bar{\Psi}_y) + \tilde{L}_{44}(\bar{F}) - \tilde{L}_{45}(\bar{N}^T) - \tilde{L}_{46}(\bar{S}^T) \\ & = \bar{I}_5 \ddot{\bar{W}}_{,y} - \bar{I}_3 \ddot{\bar{\Psi}}_y \end{aligned} \quad (1.36)$$

where all linear operators $\tilde{L}_{ij}()$ and the nonlinear operator $\tilde{L}()$ are defined by

$$\begin{aligned} \tilde{L}_{11}() &= c_1 \left[F_{11}^* \frac{\partial^4}{\partial X^4} + (F_{12}^* + F_{21}^* + 4F_{66}^*) \frac{\partial^4}{\partial X^2 \partial Y^2} + F_{22}^* \frac{\partial^4}{\partial Y^4} \right] \\ \tilde{L}_{12}() &= (D_{11}^* - c_1 F_{11}^*) \frac{\partial^3}{\partial X^3} + [(D_{12}^* + 2D_{66}^*) - c_1 (F_{12}^* + 2F_{66}^*)] \frac{\partial^3}{\partial X \partial Y^2} \\ \tilde{L}_{13}() &= [(D_{12}^* + 2D_{66}^*) - c_1 (F_{21}^* + 2F_{66}^*)] \frac{\partial^3}{\partial X^2 \partial Y} + (D_{22}^* - c_1 F_{22}^*) \frac{\partial^3}{\partial Y^3} \\ \tilde{L}_{14}() &= B_{21}^* \frac{\partial^4}{\partial X^4} + (B_{11}^* + B_{22}^* - 2B_{66}^*) \frac{\partial^4}{\partial X^2 \partial Y^2} + B_{12}^* \frac{\partial^4}{\partial Y^4} \\ \tilde{L}_{15}(\bar{N}^T) &= \frac{\partial^2}{\partial X^2} (B_{11}^* \bar{N}_x^T + B_{21}^* \bar{N}_y^T) + 2 \frac{\partial^2}{\partial X \partial Y} (B_{66}^* \bar{N}_{xy}^T) + \frac{\partial^2}{\partial Y^2} (B_{12}^* \bar{N}_x^T + B_{22}^* \bar{N}_y^T) \\ \tilde{L}_{16}(\bar{M}^T) &= \frac{\partial^2}{\partial X^2} (\bar{M}_x^T) + 2 \frac{\partial^2}{\partial X \partial Y} (\bar{M}_{xy}^T) + \frac{\partial^2}{\partial Y^2} (\bar{M}_y^T) \\ \tilde{L}_{17}() &= c_1 \left(I_5 - \frac{I_4 I_2}{I_1} \right) \left(\frac{\partial^2}{\partial X^2} + \frac{\partial^2}{\partial Y^2} \right) - I_1 \\ \tilde{L}_{21}() &= A_{22}^* \frac{\partial^4}{\partial X^4} + (2A_{12}^* + A_{66}^*) \frac{\partial^4}{\partial X^2 \partial Y^2} + A_{11}^* \frac{\partial^4}{\partial Y^4} \\ \tilde{L}_{22}() &= (B_{21}^* - c_1 E_{21}^*) \frac{\partial^3}{\partial X^3} + [(B_{11}^* - B_{66}^*) - c_1 (E_{11}^* - E_{66}^*)] \frac{\partial^3}{\partial X \partial Y^2} \\ \tilde{L}_{23}() &= [(B_{22}^* - B_{66}^*) - c_1 (E_{22}^* - E_{66}^*)] \frac{\partial^3}{\partial X^2 \partial Y} + (B_{12}^* - c_1 E_{12}^*) \frac{\partial^3}{\partial Y^3} \\ \tilde{L}_{24}() &= c_1 \left[E_{21}^* \frac{\partial^4}{\partial X^4} + (E_{11}^* + E_{22}^* - 2E_{66}^*) \frac{\partial^4}{\partial X^2 \partial Y^2} + E_{12}^* \frac{\partial^4}{\partial Y^4} \right] \\ \tilde{L}_{25}(\bar{N}^T) &= \frac{\partial^2}{\partial X^2} (A_{12}^* \bar{N}_x^T + A_{22}^* \bar{N}_y^T) - \frac{\partial^2}{\partial X \partial Y} (A_{66}^* \bar{N}_{xy}^T) + \frac{\partial^2}{\partial Y^2} (A_{11}^* \bar{N}_x^T + A_{12}^* \bar{N}_y^T) \\ \tilde{L}_{31}() &= (A_{55} - 2c_2 D_{55} + c_2^2 F_{55}) \frac{\partial}{\partial X} + c_1 (F_{11}^* - c_1 H_{11}^*) \frac{\partial^3}{\partial X^3} \\ &+ c_1 [(F_{21}^* + 2F_{66}^*) - c_1 (H_{12}^* + 2H_{66}^*)] \frac{\partial^3}{\partial X \partial Y^2} \\ \tilde{L}_{32}() &= (A_{55} - 2c_2 D_{55} + c_2^2 F_{55}) - (D_{11}^* - 2c_1 F_{11}^* + c_1^2 H_{11}^*) \frac{\partial^2}{\partial X^2} \\ &- (D_{66}^* - 2c_1 F_{66}^* + c_1^2 H_{66}^*) \frac{\partial^2}{\partial Y^2} \end{aligned}$$